Structural stability of some gold (Au) and silver (Ag) nanoparticles

MW Makgoba[a], TE Mosuang[a], MA Mahladisa[a], MG Matshaba[a], RR Maphanga[b], N Mhlanga[c], T Mokhena[c].

[a]Department of Physics, University of Limpopo, Private Bag x1106, Sovenga, 0727, South Africa.
[b]Council for Scientific industrial research/CSIR, Pretoria, South Africa, [c]Advanced Materials Division/MINTEK, Private Bag X3015, Randburg 2125, Gauteng Province, South Africa.

E-mail: **makgoba.walter@gmail.com, thuto.mosuang@ul.ac.za, rmaphanga@csir.co.za, NikiweM@mintek.co.za, TebohoM@mintek.co.za, abram.mahladisa@ul.ac.za, malili.matshaba@ul.ac.za**

Abstract. The classical molecular dynamics was used to study Au and Ag nanoparticles focusing mainly on their structural stability. The structures were modelled at various temperatures in an NVT Evans ensemble. The many-body Sutton-Chen potential was employed to describe the interactions between atoms in both nanoparticles. Variation of total energy with temperature was investigated for both Au and Ag nanoparticles; in the process, entropy was calculated. Radial distribution functions were utilised to predict the most probable Au and Ag nanoparticle structures. To probe the mobility of Au and Ag atoms in their systems, the mean square displacements (MSDs) were plotted, in which diffusion constants were calculated to be 0.58 and 1.87 Å^2/ps for Au and Ag atoms respectively at 300 K.

1. Introduction

Nanoparticles of gold (Au) and silver (Ag) have stirred up considerable scientific interest, because of their high potential for clinical applications in different areas such as biological sensing, biomedical imaging and drug delivery [1]. The outstanding potential is due to their unique physical-chemical properties, such as chemical surface functionalization, optical and electronic characteristics [1].The fascinating properties of these nanomaterials are attributed to the electronic distribution on the metal along the nanoparticle surface, which depends mostly on its size and shape that can be controlled during the synthesis procedure [1, 2]. Gold and silver nanoparticles, with various morphologies, can be fine-tuned to produce nanospheres [2], nanocubes [3], and nanorods [4].

Both gold and silver nanomaterials (AuNMs and AgNMs) can be synthesized using different methods which involve physical, chemical and biological procedures. As reported by Sttaler *et.al* [5], biologically prepared AgNMs can be obtained in abundance, with high solubility and stability probabilities when compared to the physical and chemical prepared samples. Besides, Gurunathan *et.al* [6] and Kalishwaralal *et.al* [7] commented on physically and chemically produced AgNMs as hazardous and quite expensive to fabricate. On the AuNMs front, literature suggest that Au nanorods are the most favoured on biomedical applications [8]. Despite being instrumental in drug delivery, Au nanorods can be obtained cost effectively and their synthesis methods are quite favourable. Quantitatively, according to Faraday *et.al* [9] and Davey *et.al* [10] at nanoscale both the gold and silver samples adopt the face-centred cubic (FCC) phase. In this FCC phase, thermodynamic properties of the two nanomaterials can be studied well by variation of energy, temperature, and pressure. Consequently, in this paper, the most probable Au and Ag nanospheres are being explored with the aid of the molecular dynamics approach.

2. Methodology

The classical molecular dynamics (MD) method using leapfrog verlet (LF) algorithm was used in this study. This method is one of the popular computational method that studies the physical movement of atoms and molecules [11]. It has already been established that the molecular dynamics method can simulate nanoparticles in sheets or aggregates and reveal many details of these nanomaterials that are not accessible experimentally [11]. Particularly, the DL_POLY [12] software was utilized in all the calculations. Au and Ag atoms supercells which consist of 4000 atoms each were explored at 0 K in an NVT ensemble; As a result, the convincing equilibrium structures of the supercells was attained at 48.943 and 60.121 Å respectively for both Au and Ag bulk supercells at 0 K. From these bulk supercells, the Au and Ag nanospheres were extracted for the ultimate stability analysis. The-many-body potentials such as the Sutton-Chen potential [13] was used to describe the inter-atomic interactions. Variation of total energy with temperature was investigated for the Au and Ag nanospheres. Radial distribution functions (RDFs) were utilized to predict the most probable Au and Ag-nanospheres structures while mean square displacements (MSDs) were considered to study the mobility of Au and Ag atoms in their structures.

3. Results and Discussion

3.1. Modelled Bulk Au and Ag crystals at 0 K.

Both Au and Ag precious metals can be obtained in bulk as well as nanoparticles. In this section, the possible stability of the bulk forms on these two are being discussed. The ultimate idea is to extract the nanospheres of the Au and Ag from the known properties of the bulk formations. The bulk forms of Au and Ag supercells each with 4000 atoms were modelled at 0 K using the NVT ensemble. In the process, the total energy of the supercells were observed with the changing supercell lattice constants. Figure 1, present the acquired equilibrium structures of both the Au and Ag supercells. The Au supercell lattice constant of 48.943 Å and Ag supercell lattice constant of 60.121 Å are noted in Table 1. From this data, the cohesive energies of the two were computed to be 3.673 eV/atom and 2.810 eV/atom for Au and Ag supercells respectively. Moreover, computed values agree well with experimental measurements in Table 1 [14].

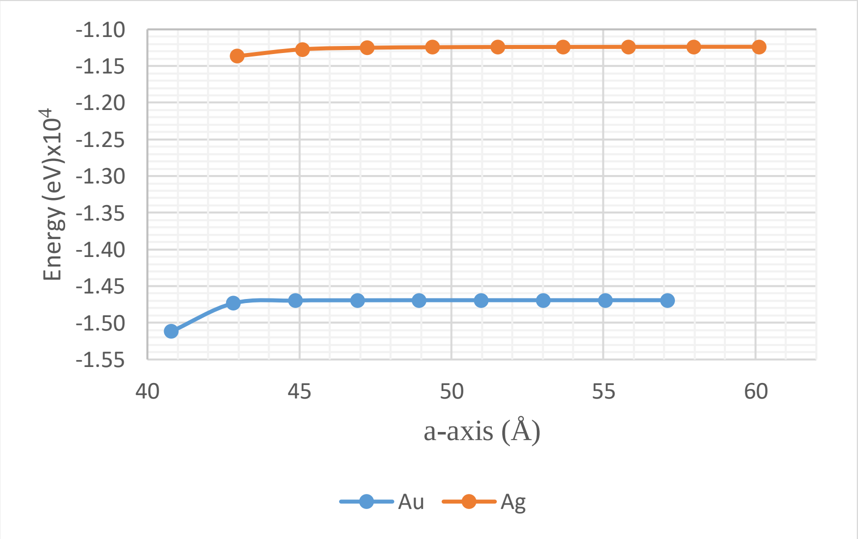

Figure 1. The graphs of energy vs a-axis for the Bulk Au and Ag structures with 4000 atoms at 0 K.

Table 1. The supercell a-axis, the total energy, the cohesive energy and its experimental reference all at 0 K for both Au and Ag bulk structures.

	$a_{supercell}$ (Å)	E_{total} (eV) x10^4	Cohesive energy (eV/atom)	Cohesive energy (eV/atom) (experimental) [14]
Au	48.943	-1.469	3.673	3.810
Ag	60.121	-1.124	2.810	2.950

3.2. Au-nanospheres and Ag-nanospheres

3.2.1. *Energy-temperature relations.* The Au-nanospheres (Au-nss) and Ag-nanospheres (Ag-nss) are extracted directly from the bulk Au and Ag supercells discussed above in section 3.1. Subsequently, the Au-nss and Ag-nss are made of 2067 atoms each with lattice constants ($a_{nanosphere}$) of 48.943 and 60.121 Å at the original 0 K. As can be seen in Figure 2, the energy increases with increasing temperature for both Au-nss and Ag-nss respectively. In this linear energy – temperature response a disjoint can be observed probable at temperature regions of 700 – 800 K and 900 – 1000 K respectively for the Au-nss and Ag-nss. Such behavior suggest the probable transition temperature in which Au-nss and Ag-nss change from one form to the other. Similar behavior of energy-temperature variation was reported by Wang *et a*l. [15] on icosahedral Au nanoparticles. Interestingly, Gafner *et al*. [16] reported a similar behavior for Cu and Ni nanoparticles. Comparable energy-temperature transitions were also reported on clusters and nanoalloys [17, 18]. To predict the entropy change of the nanospheres and possible transition temperature, energy – temperature variations were explored for both Au and Ag nanospheres as displayed in Figure 2. From these results, Table 2 displays the change in entropy for both Au-nss and Ag-nss which was found to be 7 x 10^{-4} and 8 x 10^{-4} eV/K respectively. A greater change in entropy on the Ag-nss than the Au-nss is also observed.

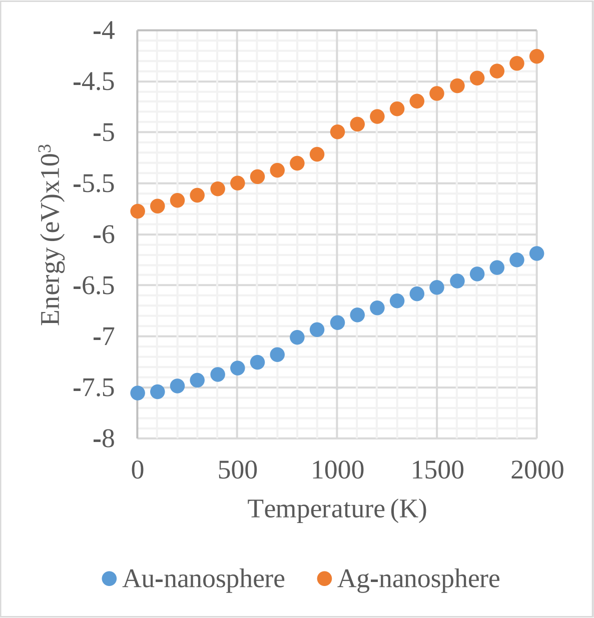

Figure 2. The variation of energy against temperature for Au- and Ag-nanospheres.

Table 2. Change in entropy for Au- and Ag-nanospheres.

	Au-nanosphere	Ag-nanosphere
Entropy (eV/K) x10^{-4}	7.000	8.000

3.2.2. *Radial distribution functions.* The radial distribution functions (RDFs) are necessary when analysing the structure of fluids and solids [19]. Researchers including Phanthania *et.al* [19] have used RDFs for the analysis of fluid structures. For this reason, the RDFs have been utilized on identifying a possible phase change of Au-nss and Ag-nss over a prescribed temperature range. In Figure 3 (a) and (b), the RDFs at 300, 600, 700, and 800 K for the Au-nss and Ag-nss respectively are presented. In the plots, it can be seen that the peak heights (g(r)) decrease with the increasing temperature, as well as diminishing with the increasing radial distance (r). The trend suggest a possible phase transition from solid to fluid state. For instance, on the Au-nss at 800 K, only the first and second nearest neighbor Au – Au displacements can be described with slight uncertainty (Figure 3(a)) in position. This observation seems to support the energy – temperature relation observed in Figure 2. Using the similar argument and observations on the Ag-nss, the projected phase transition temperature could be in the region of 900 – 1000 K.

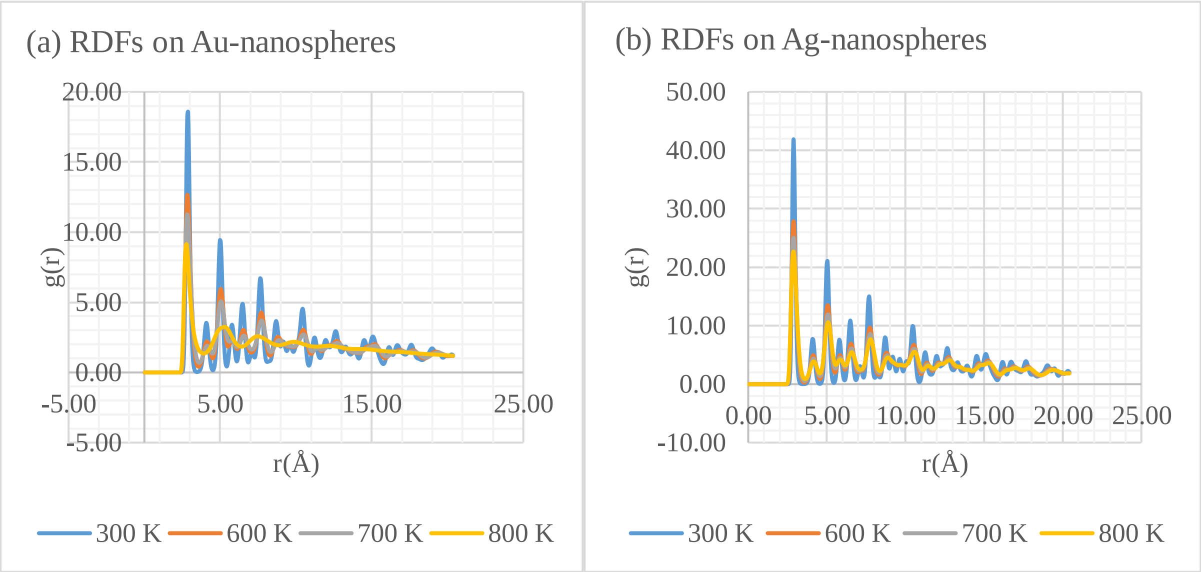

Figure 3. The radial distribution functions (RDFs) for Au- (a) and Ag-nanospheres (b).

3.2.3. *Mean square displacements.* Mean square displacements (MSDs) have been utilised to describe the movement of atoms in solids, liquids as well as gases [20]. Therefore, it has been reported that the MSDs will increase linearly with relation to time when diffusion takes place [20]. As such, to probe the mobility of the Au and Ag ions in their Au-nss and Ag-nss systems respectively, the mean square displacements (MSDs) plots were constructed. From such MSDs plots, the respective ions diffusion constant were calculated. Figures 4 (a) – (b), illustrates the MSDs graphs of Au-nss and Ag-nss respectively at 300, 600, and 700 K. The values of the calculated diffusion constants are displayed in Table 3. For Au ions the diffusion constants increase with increasing temperature. In the case of Ag-nss, the diffusion constants seems to decrease with the increasing temperature. This should not come as a surprise since the chosen temperature range is far from the suggested transition temperature for the Ag-nss.

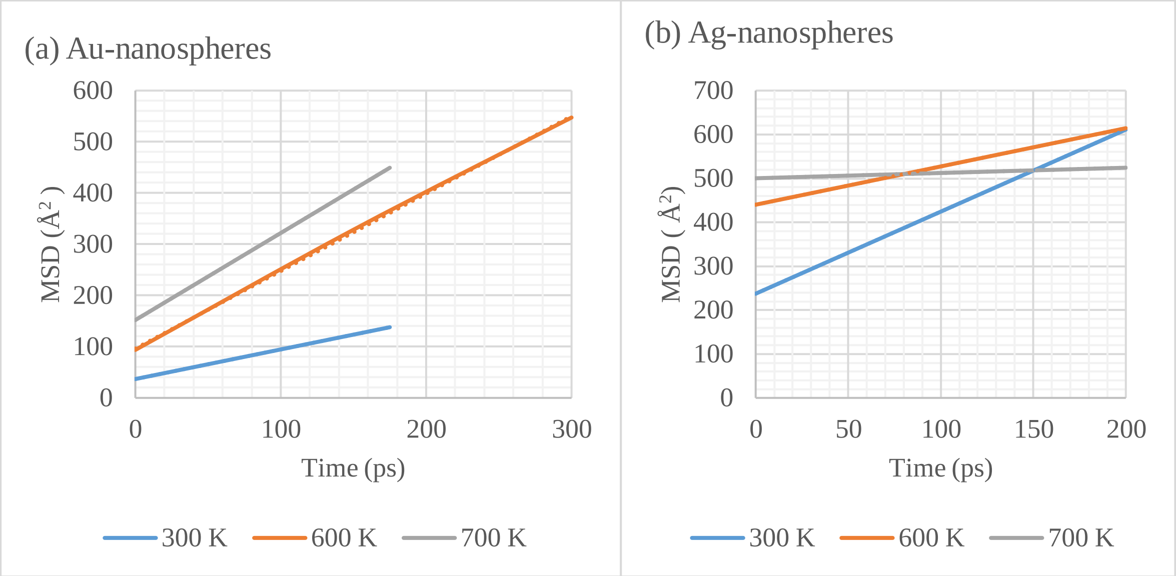

Figure 4. Mean square displacements for Au- (a) and Ag-nanospheres (b).

Table 3. Diffusion constants for Au- and Ag-nanospheres.

Temperature (K)	300	600	700
Diffusion constant (D) for Au-nanospheres (Å^2/ ps)	0.58	1.46	1.70
Diffusion constant (D) for Ag-nanospheres (Å^2/ ps)	1.87	0.87	0.12

4. Conclusion

In the radial distribution functions (RDFs), the height of the peaks decreases with an increase in temperature followed by the number of peaks. Hence, the transition from solid to liquid can successfully be traced through the radial distribution functions. It can be concluded that Au-nanopspheres show quick melting point at 800 K as compared to Ag-nanospheres. The mobility of the Au and Ag ions was satisfactorily described and tracked through the mean square displacements graphs, in which the mobility of Au atoms was found to increase with an increase in temperature and vice versa for the mobility of Ag atoms. As such, the stable structures of Au and Ag nanospheres are accumulated at low temperatures or below transition temperature. The transition temperature, change in entropy and the diffusion constants all suggests that the Au-nanospheres phase transformation is obtained readily than Ag-nanospheres.

References

[1] Elahi N and Kamali M, *a review Talanta*, **184** (2018), pp. 537-556.
[2] Link S and El-Sayed M A, *J. Phys. Chem. B,* **103** (1999), pp. 4213-4214.
[3] Sun Y and Xia Y, *J. American Chem. Soc*., **126** (2004), pp. 3893-3895.
[4] Cepak V M and Martin C R, *J. Phys. Chem. B,* **102** (1998), pp. 9985-9990.
[5] Sttaler K, Mu hlbach J and Recknagel E, *Phys. ReV. Lett.*, **45** (1980), pp. 821-824.
[6] Gurunathan S, Park J H, Han J W and Kim J H, *Int. J. Nanomed.* **10** (2015), pp. 4203-4222.
[7] Kalishwaralal K, Gurunathan S, Vaidyanathan R, Venkataraman D, Pandian S R, Muniyandi J, Hariharan N and Eom S H, *Colloids Surf. B Biointerfaces*. **74** (2009), pp. 328-335.
[8] Jiang X M,Wang L M, Wang J and Chen C Y, *Appl. Biochem. Biotechnol*, **166** (2012), pp. 1533-1551.
[9] Faraday M, *Philos. Trans. R. Soc. Lond.* **147** (1857), pp. 145-181.
[10] Davey W P, *Phys. Rev*. **25** (1925), pp. 753-761.
[11] Frenkel D and Smit B, Understanding Molecular Simulation. 2nd ed., Academic, San Diego (2002).
[12]Smith W, Forester T R and Todorov I T, The DL_POLY 2 User Manual, STFC Daresbury Laboratory, Daresbury, Warrington WA4 4AD Cheshire, UK (2009).
[13] Sutton A P and Chen J, *Phil. Mag. Lett*. **61** (1990) pp. 139-146.
[14] Kimura Y, Qi Y, Cagin, T and Goddard W A III, Caltech ASCI Technical Report (1998).
[15] Wang Y, Teitel S and Dellago C, *Chem Phys Lett.* **394** (2004), pp. 257-261.
[16] Gafner S L, Redel L V, and Gafner Yu Ya, *J. Comput. Theor. Nanosci*. **6** (2009), pp. 820-827.
[17] Baletto F, Mottet C and Ferrando R, *Chem Phys Lett.* **354** (2002), pp.82-87.
[18] Pavan L, Baletto F and Novakovic R, *Phys. Chem. Phys.* **17** (2015), pp. 28364-28371.
[19] Pathania Y and Ahluwalia P K, *J. Phys.,* **65** (2005), pp. 457-468.
[20] Gao F and Qu J, *Mater. Lett.* **73** (2012), pp. 92-94.